

High field-effect mobility ZnO thin-film transistors with Mg-doped Ba_{0.6}Sr_{0.4}TiO₃ gate insulator on plastic substrates

KyongTae Kang, Mi-Hwa Lim, Ho-Gi Kim, Il-Doo Kim, and Jae-Min Hong

Citation: *Appl. Phys. Lett.* **90**, 043502 (2007); doi: 10.1063/1.2434150

View online: <http://dx.doi.org/10.1063/1.2434150>

View Table of Contents: <http://apl.aip.org/resource/1/APPLAB/v90/i4>

Published by the [American Institute of Physics](#).

Additional information on *Appl. Phys. Lett.*

Journal Homepage: <http://apl.aip.org/>

Journal Information: http://apl.aip.org/about/about_the_journal

Top downloads: http://apl.aip.org/features/most_downloaded

Information for Authors: <http://apl.aip.org/authors>

ADVERTISEMENT



Goodfellow
metals • ceramics • polymers • composites
70,000 products
450 different materials
small quantities fast

www.goodfellowusa.com

High field-effect mobility ZnO thin-film transistors with Mg-doped Ba_{0.6}Sr_{0.4}TiO₃ gate insulator on plastic substrates

KyongTae Kang, Mi-Hwa Lim, and Ho-Gi Kim

Department of Materials Science and Engineering, Korea Advanced Institute of Science and Technology, Daejeon 305-701, Republic of Korea

Il-Doo Kim^{a)} and Jae-Min Hong

Optoelectronic Materials Research Center, Korea Institute of Science and Technology, P.O. Box 131, Cheongryang, Seoul 130-650, Republic of Korea

(Received 21 September 2006; accepted 19 December 2006; published online 23 January 2007)

The authors report on the influence of Mg acceptor doping on the markedly reduced leakage current characteristics ($<5 \times 10^{-8}$ A/cm² at 2 MV/cm) of Ba_{0.6}Sr_{0.4}TiO₃ thin films. The suitability of room temperature deposited Mg-doped Ba_{0.6}Sr_{0.4}TiO₃ films as gate insulators for low-voltage ZnO thin-film transistors (TFTs) (<6 V) was investigated. All room temperature processed ZnO-TFTs on plastic substrates exhibited a high field-effect mobility of 16.3 cm²/V s and a current on/off ratio of 6.4×10^4 . The threshold voltage and subthreshold swing were 2.8 V and 400 mV/decade, respectively. © 2007 American Institute of Physics. [DOI: 10.1063/1.2434150]

ZnO thin-film transistors (TFTs) have attracted much attention due to their potential of replacing hydrogenated amorphous or polycrystalline silicon (*a*-Si:H or poly-Si) TFTs.¹ ZnO is a transparent compound semiconductor with a wide band gap (3.37 eV) which can be grown as a polycrystalline film at room temperature. Therefore, ZnO is considered to be an ideal material for serving as the channel layer in transparent and flexible TFTs.¹⁻³ So far, considerable efforts have been done to obtain high-performance ZnO (or doped ZnO)-TFTs with a high field-effect mobility (1–80 cm²/V s) and high on/off ratios (10⁵–10⁷).^{4,5} However, large threshold and high operating voltages are still a major limitation for portable, battery-powered applications. In order to drive high operating current at low bias voltages, high-*k* gate dielectrics of more than 200 nm thickness (pinhole-free and good step coverage) are normally needed to increase the capacitive coupling between gate electrode and active channel. However, a common limitation of near room temperature deposited high-*k* dielectrics, e.g., Bi_{1.5}Zn_{1.0}Nb_{1.5}O₇,¹⁻³ barium zirconium titanate,⁶ HfO₂,⁷ and TiO₂,⁸ is their tendency to suffer from high leakage currents, detrimental to ZnO-TFTs operation. As a potential candidate for gate insulators, we recently developed Mn-doped Ba_{0.6}Sr_{0.4}TiO₃ (BST) thin films deposited at room temperature.⁹ Mn-doped BST films could provide the requisite high dielectric constant (~ 24) coupled with enhanced leakage current characteristics. However, Mn, which occupies the Ti site (Ti⁴⁺, $r_{\text{eff}}=0.605$ Å) of the BST perovskite structure, has multivalence states with ionic radii between Mn²⁺ ($r_{\text{eff}}=0.67$ Å) and Mn⁴⁺ ($r_{\text{eff}}=0.53$ Å) in a sixfold coordination. If an electron acceptor with lower single valence state, i.e., Mg²⁺ ($r_{\text{eff}}=0.72$ Å), is used, further reduction in the leakage current density can be achieved due to the deep trapping of electrons that would be normally generated in the Ti derived three-dimensional-like conduction band.¹⁰ In this letter, we report on the role of Mg acceptor doping on markedly reduced leakage current characteristics of room temperature grown BST thin films. The suitability of 3% Mg-

doped BST films as gate insulators for the fabrication of high-performance ZnO-TFTs on a polyethylene terephthalate (PET) substrate is discussed.

Disk-type undoped BST, 3% Mg-doped BST, and ZnO targets were prepared by a conventional mixed oxide method. 200 nm thick undoped and 3% Mg-doped BST thin films were grown on Pt/Ti/SiO₂/Si substrates by rf magnetron sputtering using a power (100 W), working pressure (50 mTorr), and an Ar/O₂ (ratio=10/10) atmosphere at room temperature. For electrical measurement, Pt electrodes (area=2×10⁻⁴ cm²) of 100 nm thickness were formed through a shadow mask on undoped and 3% Mg-doped BST films by dc magnetron sputtering. The valence states of Mg in BST films were characterized with x-ray photoelectron spectroscopy (XPS). The dielectric properties were measured at 100 kHz with an applied voltage up to 10 V using an HP4192A impedance analyzer. Current-voltage (*I*-*V*) characteristics were examined with an HP4145B semiconductor parameter analyzer.

XPS measurements were carried out with a PHI 5800 ESCA system using a monochromator Al *K*α with an energy of 1486.6 eV and a spot size of 400×400 μm². The energy scale of the XPS spectra was calibrated with C 1s at 284.6 eV. In order to demonstrate the advantages of 3% Mg-doped BST films as gate insulators, ZnO-TFTs were fabricated on PET substrates. Figure 1 shows a schematic cross-sectional view of our device. First, a 100 nm thick Cr gate

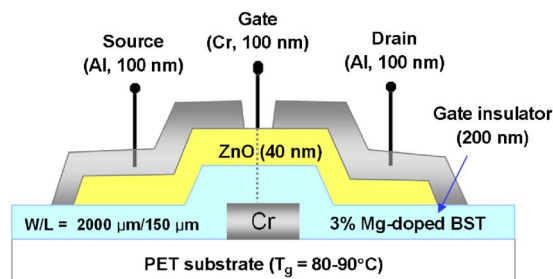


FIG. 1. (Color online) Schematic cross-sectional view of ZnO-TFT structure with 200 nm thick 3% Mg-doped BST gate insulator.

^{a)}Electronic mail: idkim@kist.re.kr

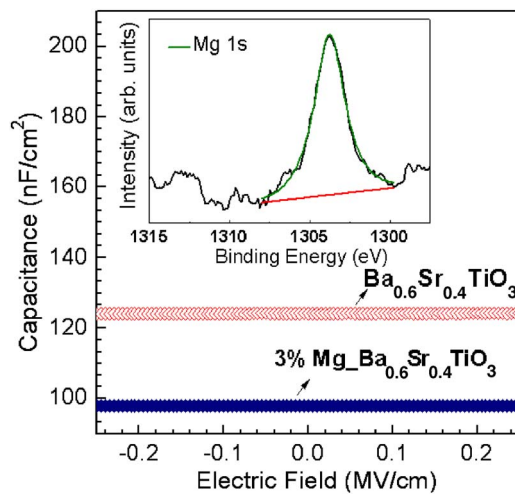


FIG. 2. (Color online) Capacitance per unit area–electric-field characteristics of pure BST and 3% Mg-doped BST films with the configuration of metal-insulator-metal (MIM) structure.

electrode was deposited by rf sputtering with the aid of a shadow mask. A 200 nm thick 3% Mg-doped BST gate insulator was then deposited onto the Cr covered PET substrates by rf sputtering. A ZnO *n*-type channel layer was subsequently deposited at room temperature by sputtering using a rf power (115 W), working pressure (50 mTorr), and an Ar [20 SCCM (SCCM denotes cubic centimeter per minute at STP)] atmosphere to a thickness of 40 nm. Transistors were completed by the evaporation of Al top contacts through shadow masks so as to obtain a channel length of 150 μm and a width of 2000 μm .

Figure 2 shows the capacitance-density–electric-field characteristics of the BST and 3% Mg-doped BST films measured in a metal-insulator-metal (MIM) configuration. The measured capacitance per unit area, for a pure BST film of 200 nm thickness, was 124 nF/cm² at 100 kHz. The capacitance corresponds to a relative dielectric constant of 28. Compared to the undoped BST films, 3% Mg-doped BST films exhibited a slightly lower dielectric constant of 22. The effective dielectric constant ($\epsilon_r \sim 22$) of the 3% Mg-doped BST films remained still high enough to achieve a low-voltage operation of less than 6 V in the ZnO-TFTs. In particular, no measurable tunability was observed up to voltages of 0.25 MV. These paraelectric behaviors, i.e., negligible voltage independent capacitance tunability, of 3% Mg-doped BST films can provide more predictable operation in terms of higher stability and lower hysteresis characteristics for the ZnO-TFTs.

In order to investigate the existence of Mg acceptor in the BST matrix, we carried out XPS analysis. We observed the Mg 1s spectra in XPS (inset of Fig. 2). This result indicates that Mg was well doped within the BST matrix. For Mg 1s spectra in XPS, the peak position was recorded in a range of 1303.5–1304.1 eV. The corresponding Mg–O peak position for Mg 1s is 1303.8 eV. The peak position is well matched with the measured Mg 1s peak position. This result demonstrates that Mg could serve as an electron acceptor with chemical bonding of Mg–O in the BST matrix. Based on the XPS result, i.e., valence state of Mg²⁺, we could use Kröger-Vink notation to describe electrical charge and lattice position for defect species (Mg²⁺) in BST films.

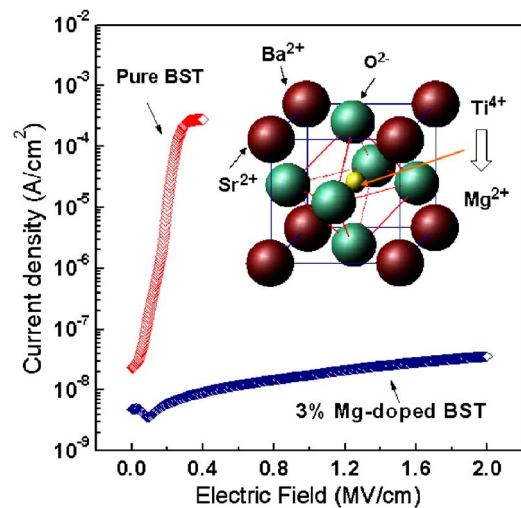
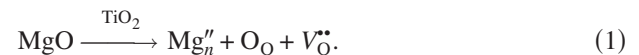
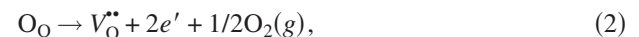


FIG. 3. (Color online) Current-density–electric-field characteristics of pure BST and 3% Mg-doped BST films. The inset shows a schematic structure for Mg substitution into Ti site in BST lattice.

Figure 3 shows the *I*-*V* characteristics of pure BST and 3% Mg-doped BST thin films as a function of applied bias voltage. The undoped BST thin films showed poor leakage current properties, i.e., low breakdown strength at 0.4 MV/cm.³ On the other hand, the measured leakage current density of the 3% Mg-doped BST films remained on the order of $\sim 2\text{--}3 \times 10^{-8}$ A/cm² even up to an applied electric field of 2 MV/cm (40 V), thereby demonstrating significant improvement in leakage current characteristics. The lower leakage current in the 3% Mg-doped BST films can be attributed to the acceptor behavior of Mg, which partially substitutes for Ti on the B site of the $A^{2+}B^{4+}O_3^{2-}$ perovskite structure. The inset shows a schematic structure for Mg substitution into Ti site in BST lattice. On the basis of the similar ionic radii between Ti⁴⁺ ($r_{\text{eff}} = 0.605 \text{ \AA}$) and Mg²⁺ ($r_{\text{eff}} = 0.72 \text{ \AA}$) in the sixfold coordination, we assume that Ti⁴⁺ can be replaced by Mg²⁺. Negatively charged defects (Mg_{Ti}^{••}) and a corresponding number of doubly ionized oxygen vacancy ($V_{\text{O}}^{\bullet\bullet}$) are simultaneously formed to satisfy the site balance and charge neutrality, i.e.,



In this case, Mg behaves as an acceptor-type dopant and prevents reduction of Ti⁴⁺ to Ti³⁺ by neutralizing the donor action of the oxygen vacancies. During the BST film growth, a reduction process may result in a *n*-type conductivity in the prepared films according to the following equation:



where O_O, V_O^{••}, and *e'* represent the oxygen ion on its normal site, the oxygen vacancy, and electron, respectively. The increase in the oxygen vacancy concentration created by MgO addition eventually causes a decrease in the concentration of electrons. In accordance with these arguments, the leakage current density of Mg-doped BST film was markedly reduced, as shown in Fig. 3. Although 3% Mg-doped BST films showed a noncrystalline structure (not shown), it is expected to have a local short-range ordering in 3% Mg-doped BST films.² Therefore, the defect notation which was described by simple substitution of Mg²⁺ for Ti⁴⁺ in Eqs. (1) and (2) might be used to explain the remarkable reduction of

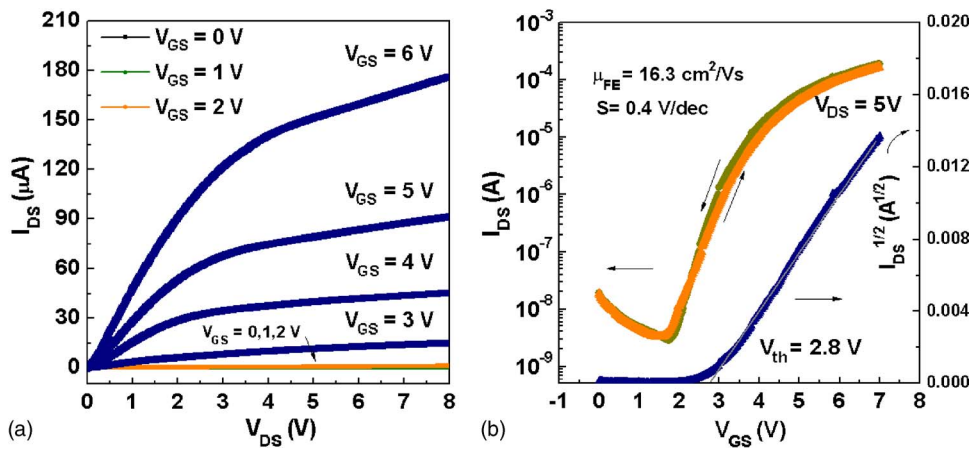


FIG. 4. (Color online) (a) Drain-to-source current (I_{DS}) vs drain-to-source voltage (V_{DS}) curves at various gate-to-source voltages (V_{GS}) for ZnO-TFTs with 3% Mg-doped BST gate insulators on PET substrates. [A channel length (L) of 150 μm and a channel width (W) of 2000 μm .] (b) Transfer characteristics. V_{GS} was swept from 0 to 7 V at V_{DS} of 5 V.

leakage current density. Further study is needed to confirm it.

Figure 4(a) shows the drain-to-source current (I_{DS}) as a function of drain-to-source voltage (V_{DS}) at various gate voltages of ZnO-TFTs with 3% Mg-doped BST gate insulators on a PET substrate. All ZnO-TFTs were prepared at room temperature due to the low glass transition temperature (T_g) of 80~90 $^{\circ}\text{C}$. The relatively high capacitance of the 3% Mg-doped BST gate insulators resulted in a low-voltage operation of less than 6 V. Good current saturation and high on current of 160 μA at the bias condition (e.g., V_{GS} and V_{DS} =6 V) were observed. Figure 4(b) shows the transfer characteristics of the ZnO-TFTs. The threshold voltage (V_{th}) was calculated from the x -axis intercept of the square root of the I_{DS} vs V_{GS} plot. Field-effect mobility (μ_{FE}) modeled by the equation $I_{DS} = (WC_i/2L)\mu_{FE}(V_{GS} - V_{th})^2$ can be calculated from the slope of the plot of $|I_{DS}|^{1/2}$ vs V_{GS} in the saturation region (V_{GS} =5 V), where L is the channel length, W is the channel width, C_i is the capacitance per unit area of the insulating layer, V_{th} is the threshold voltage, and μ_{FE} is the field-effect mobility. The measured V_{th} and μ_{FE} were +2.8 V and 16.3 $\text{cm}^2/\text{V s}$ for the ZnO-TFTs with 3% Mg-doped BST gate insulators, respectively. The measured subthreshold swing was 400 mV/decade. On-current and off-current were 1.86×10^{-4} and 2.90×10^{-9} A, respectively, giving an on/off current ratio of 6.4×10^4 . In particular, it is interesting to note that there is no detectable hysteresis behavior in the dc gate characteristics when sweeping V_{GS} in the forward and reverse directions, as shown in Fig. 4(b). It suggests negligible charge traps for ZnO/3% Mg-doped BST stack. In general, high- k gate insulators exhibit counterclockwise hysteresis loops in I_{DS} - V_{DS} characteristics due to the ferroelectric or nonlinear dielectric nature of gate insulators. This result indicates that high quality 3% Mg-doped BST gate

insulators could be obtained even at room temperature deposition.

In summary, 3% Mg-doped BST films with a high dielectric constant ($\epsilon_r \sim 22$) and low leakage current property ($< \sim 5 \times 10^{-8}$ at 2 MV/cm) were prepared at room temperature by rf sputtering. A remarkable reduction in leakage current density could be achieved through deep trapping of electrons in 3% Mg-doped BST films. All room temperature processed ZnO-TFTs on PET substrates using the 3% Mg-doped BST gate insulators (200 nm) exhibited a low-voltage operation of less than 6 V and a high field-effect mobility of 16.3 $\text{cm}^2/\text{V s}$. These results demonstrate the potential use of 3% Mg-doped BST gate insulators for producing high-performance ZnO-TFTs on plastic substrates.

This work was supported by a KIST independent project of one of the authors (I.-D.K.).

- ¹I. D. Kim, Y. W. Choi, and H. L. Tuller, Appl. Phys. Lett. **87**, 042509 (2005).
- ²I. D. Kim, M. H. Lim, K. T. Kang, H. G. Kim, and S. Y. Choi, Appl. Phys. Lett. **89**, 022905 (2006).
- ³Y. W. Choi, I. D. Kim, H. L. Tuller, and A. I. Akinwande, IEEE Trans. Electron Devices **52**, 2819 (2005).
- ⁴H. Yabuta, M. Sano, K. Abe, T. Aiba, T. Den, H. Kumomi, K. Nomura, T. Kamiya, and H. Hosono, Appl. Phys. Lett. **89**, 112123 (2006).
- ⁵J. Siddiqui, E. Cagin, D. Chen, and J. D. Phillips, Appl. Phys. Lett. **88**, 212903 (2006).
- ⁶C. D. Dimitrakopoulos, S. Purushothaman, J. Kymissis, A. Callegari, and J. M. Shaw, Science **283**, 822 (1999).
- ⁷P. F. Carcia, R. S. McLean, and M. H. Reilly, Appl. Phys. Lett. **88**, 123509 (2006).
- ⁸L. A. Majewski, R. Schroeder, and M. Grell, Adv. Mater. (Weinheim, Ger.) **17**, 192 (2005).
- ⁹K. T. Kang, M. H. Lim, H. G. Kim, Y. Choi, H. L. Tuller, I. D. Kim, and J. M. Hong, Appl. Phys. Lett. **87**, 242908 (2005).
- ¹⁰J. Y. Kim, C. R. Song, and H. I. Yoo, J. Electroceram. **1**, 27 (1997).